Bulg. J. Phys. 42 (2015) 544–553

Systematic Evaluation of the Nuclear Binding Energies as Functions of F-spin

A.I. Georgieva[1], **A. Aprahamian**[2], **I. Bentley**[2,3],
A. Teymurazyan[2], **A. Nystrom**[2]
[1]Institute of Solid State Physics, Bulgarian Academy of Sciences,
Sofia 1784, Bulgaria
[2]Dept. of Physics, University of Notre Dame, Notre Dame, IN 46556
[3]Dept. of Chemistry and Physics, Saint Mary's College, Notre Dame, IN 46556

Received *30 October 2015*

Abstract. A smooth dependence of the microscopic component of the nuclear binding energy on the third projection of the F-spin and the proton number is obtained by an application of a generalized $Sp(4, R)$ classification scheme of even-even nuclei within the major nuclear shells. The results are compared with the ones from a systematic of nuclear masses in respect to the promiscuity factor (P) and the relation of the later and the F-spin projection is established, which further motivates the obtained empirical result.

PACS codes: 21.10.Dr,21.60.-n,21.60.Cs

1 Introduction

Atomic masses are one of the most important nuclear characteristics and are widely used in basic nuclear physics and astrophysics. Hence, since the beginning of the studies in the nuclear structure physics the problem of creating a reliable nuclear mass models was addressed both in macroscopic and microscopic approaches. Macroscopic models [1, 2] based on treating the nucleus as a liquid drop, often depend on macroscopic parameters like proton number (Z), neutron number (N), atomic mass number $(A = N + Z)$, and contain some additional coefficients, which are fit. Microscopic models [3, 4] based on the shell model, account for the interactions between individual nucleons. This is typically done employing Skyrme (e.g. [5]) or pairing interactions [6], or applying the BCS approximation [7]. Recently, a combination of the two (e.g. [8–12]) is used more often, but comparing the results from them it is clear that these models typically deviate substantially in regions, where the experimental data were not fit and diverge relatively quickly as one moves away from the valley of stability.

Other approaches to predicting masses make use of finding and fitting observed trends in their behavior. Garvey-Kelson relations involve determining the mass of a nucleus using several nearby neighbors [13]. It has been suggested that these relationships can be used to test mass formulas in an attempt to make more accurate predictions [14]. Comparable approaches have been used to approximate the residual valence proton-neutron interaction [15].

Evaluations of the nuclear masses along isobaric chains using a quadratic polynomial expansion in isospin projection ($T_Z = (N - Z)/2$) has long been used (see [16] or [17]). The Isobaric Mass Multiplet Equation (IMME) can be used as a predictive tool for determining the binding energy of unmeasured nuclei (e.g. [18, 19]). Precision measurements, initially for low mass nuclei and modern Penning trap measurements of mid-mass nuclei, have verified that higher order terms are necessary, see e.g. [20, 21]. Fitting procedures, like the IMME, typically have a localized use, filling in a missing mass, only predicting masses along an isobaric/isotopic chain and therefore do not have the ability to predict global characteristics.

We propose an alternative approach which is a hybrid combination of a mass model and fitting technique. We propose a mass model to determine the macroscopic contribution and determine the microscopic correlations, by means of empirically fitting nuclei within specific nuclear shells. This approach allows for broader scope than is typical at present. The aim of it is to provide more accurate predictions of masses in regions where the masses of nearby nuclei are known and to point out at the necessity to additionally measure with higher precision some masses, which don't follow the observed trends.

2 Classification Scheme and Empirical Investigation of the Semi-Empirical Microscopic (SEM) Masses

It is clear, that an empirical investigation of specific nuclear properties like the excited or the binding energies in the nuclear spectra, will be of great help for the development of future experiments, that will test the theory and outline its limits of application. Such an investigation is best done in the framework of a systematic, which is based upon the nuclear characteristics on which the trends in the behavior of the investigated nuclear observables are clearly seen [22].

From theoretical point of view, it is of great importance to provide a reliable nuclear characteristics, that specify in a best way the observed phenomena. In [23], based on the appropriate classification [24] of the nuclei belonging to a major nuclear shell and the observed smooth behavior of their yrast energies as functions of the classification numbers, the authors were able to derive a general phenomenological formula describing this behavior rather accurately. In the present investigation we would like to test the advantages of this classification scheme in the evaluation of the nuclear masses.

We start with an empiric investigation of the existing data on the nuclear binding energies in terms of the already used $sp(4, R)$ classification scheme [23]. As with the previous study, this investigation is aimed at gaining an empirical understanding of the trends in the behavior of these binding energies. This scheme is particularly useful since it combines a consideration of the microscopic structure of nuclei with simple but general symmetry principles. The employed classification scheme depends only on two classification numbers:

$$N_t = (N_\pi + N_\nu), \text{ and } F_0 = \frac{1}{2}(N_\pi - N_\nu), \tag{1}$$

where

$$N_\pi = \frac{1}{2}(Z - Z_{\min}), \text{ and } N_\nu = \frac{1}{2}(N - N_{\min}), \tag{2}$$

which depend on the magic numbers. The (min) value corresponds to the shell closure in which the nucleons are at or immediately above. For protons: $Z_{\min} = [8, 20, 28, 50, 82]$, and for neutrons: $N_{\min} = [8, 20, 28, 50, 82, 126]$. Please note that Eq. (2) is identical to the definition in the well known proton-neutron version of the Interacting Boson Model (IBM) often referred to as the IBM-2 [25]. The physical interpretation of the introduced eigenvalues of the algebraic operators in both cases is the same. These two operators give the number of proton and neutron valence pairs within a given shell beyond their respective closed cores (the usual magic numbers denoted here by $Z_{\min}$ and $N_{\min}$) which serve as the vacuum state of the system. Each of the nuclei considered in this study has a unique N_t and F_0 value. One important development in this paper is the use of a generalized expression for F_0, so that it also includes odd numbers of valence nucleons.

Next we consider also one of the most successful classifications of nuclear properties [26], which is based on the introduction of the promiscuity factor (P), which has been shown to describe collectivity regardless of the deformation or mass region [27]. It is a measure of the average number of proton-neutron interactions per a valence nucleon and is defined as:

$$P = \frac{N_p N_n}{N_p + N_n}, \tag{3}$$

where N_p and N_n are counted as the numbers of particles or holes for protons or neutrons depending on if the shell is less than or more than half full, respectively.

It is possible to obtain the dependence of the nuclear parameter P on the characteristics N_t and F_0. For the parameter P it is easy to obtain the relation:

$$P = \frac{1}{2N_t}\{(N_t)^2 - 4(F_0)^2\}. \tag{4}$$

Accordingly from (4) $(F_0)^2$ is expressed as a function of N_t and P

$$F_0^2 = \frac{N_t}{2}\left(\frac{N_t}{2} - P\right). \tag{5}$$

The obtained expression looks like the eigenvalue of the generalized pairing interaction, which is particularly important in the light nuclear shells. It should be pointed out, that the quantity P is not defined at shell closures, however F_0 is defined there [24]. The classification schemes are applied for the empirical investigation of the Semi-Empirical Microscopic masses (SEM), from [28], which are defined as:

$$SEM = ME_{Exp} - E_{MAC}. \quad (6)$$

In Eq. (6) the experimentally determined mass excess (ME_{Exp}) are taken from 2012 Atomic Mass Evaluation /AME/ tables [29], and hence we use the notation SEM_{12}. Extrapolated masses in the AME tables are not used in the determination of the experimental SEM.

In this work, we have chosen to use the macroscopic energy (E_{MAC}) from the Finite Range Droplet Model (FRDM) of Möeller, Nix et al. [8]. The residual microscopic part of the nuclear masses SEM contains the structure and deformation dependence, which is best studied in the above mentioned systematics, related to the valence nuclear shells.

In Figure 1 we present an empirical investigation of the behavior of the SEM_{12}, in a systematic based on P and F_0. The SEM_{12} values appear to stabilize at about 4 MeV for moderately large values of $P \gtrsim 3$, which is consistent with [27]. The P term is not defined for nuclei with a closed shell for the proton or neutron systems. To allow for further investigation, the seemingly constant SEM, seen for large values of P, will not be used. Instead a quadratic relationship for F_0 can be used to fit the mass excesses for all nuclei. The right panel of Figure 1 includes the SEM_{12} values plotted as a function of F_0 where SEM show a rather smooth and regular behavior for the isotopic chains belonging to this shell zone. Consequences of the sub-shell closures are demonstrated in the SEM_{12} as a dip downward seen in some nuclei.

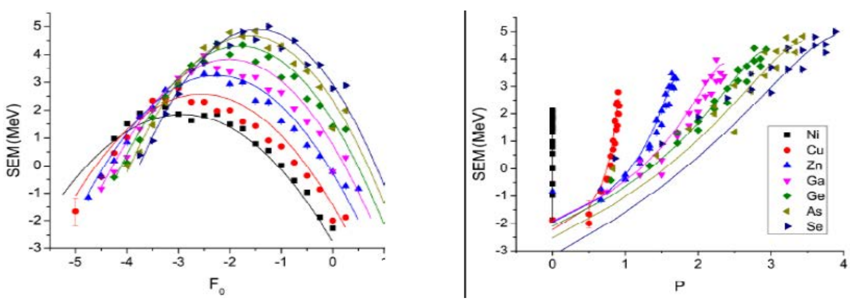

Figure 1. (Color on-line) The SEM using the macroscopic portion of the Finite Range Liquid Drop Model [8] and the AME 2012 [29] as a function of F_0 and P for the nuclei consisting of $28 \leq Z \leq 34$ and $28 \leq N \leq 49$.

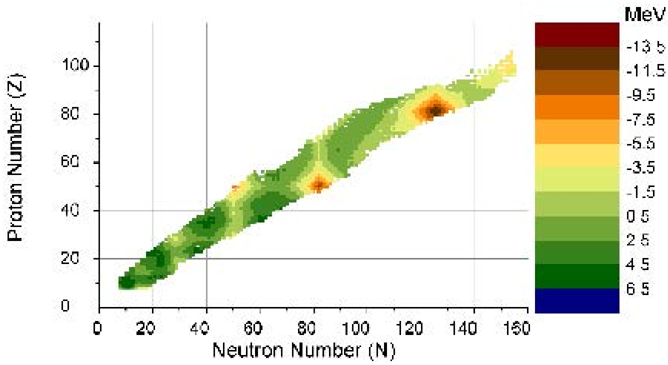

Figure 2. (Color on-line) The SEM determined using (6), which contains the mass excess from AME 2012 [29] and the macroscopic energy from the Finite Range Liquid Drop Model [8].

Figure 2 is a plot of SEM_{12} on the chart of the nuclides which demonstrates that the microscopic portion contains features related to shell effects. More specifically, at shell closures the SEM goes to a relative minimum, which appears to become deeper for the heavier shells. Towards the middle of the shells the values of SEM increase, with the increase of deformation, which confirms that the behavior observed in Figure 1 is similar for all other shells and possibly more pronounced in heavier shells.

3 Dependence of SEM on F_0

The proton-neutron interaction is known to be very important when the valence protons and neutrons are in the same shell, and substantially less important, if the valence nucleons are in differing shells. In [30] the empirical investigation based on the $Sp(4,R)$ classification of the nuclear SEMs in the major nuclear shell with proton numbers $28 < Z < 50$ and neutron numbers $28 < N < 50$ showed as a good approximation for the SEM to be a function of the product of quadratic expansions of F_0 with coefficients a quadratic expansion on Z. This defines $\text{SEM}_{F-\text{Spin}}$ as a function of nine coefficients in the following way:

$$SEM_{F-\text{Spin}} = (B_{00} + B_{01}Z + B_{02}Z^2) \qquad +(B_{10} + B_{11}Z + B_{12}Z^2)F_0 + (B_{20} + B_{21}Z + B_{22}Z^2)F_0^2. \tag{7}$$

F_0 is determined using Equations (1) and (2). Therefore F_0 is a function of the place of the nucleons in the nuclear shells.

In this paper, we fit the coefficients in (7) for each of the shells defined by the magic numbers $Z_{\min} = [8, 20, 28, 50, 82]$, and $N_{\min} = [8, 20, 28, 50, 82, 126]$, separately. There are 10 shells which contain a sufficient number of nuclei to perform the nine parameter fit. Moreover in the fitting procedure we account for the following sub-shell closures:

- at $Z = 14$ and $N = 16$ (see e.g. [31] or [32])
- at $Z = 64$, and $N = 90$ (e.g. [33])
- at $N = 90$, based on a theoretical consideration treating the $g9/2$ neutrons differently than the others.

Hence hereafter we present results for 15 zones which are used in the fits and are presented in Table 1, where the bold numbers indicate the sub-shell closures used. In the last column of the table, the number of experimentally observed binding energies given in AME_{12} [29] and used in the fitting procedure are given.

Table 1. F-Spin Zones

Zone	$Z_{\min}$	$Z_{\max}$	$N_{\min}$	$N_{\max}$	Number in AME_{12} [29]
1a	8	19	8	**15**	64
1b	8	19	**16**	19	47
2	8	19	20	27	63
3	20	27	20	27	53
4	20	27	28	49	88
5	28	49	28	49	241
6	28	49	50	81	327
7	50	81	50	81	297
8a	50	**63**	82	**89**	102
8b	50	**63**	**90**	102	62
8c	**64**	81	82	**89**	79
8d	**64**	81	**90**	125	420
9	82	125	82	125	161
10a	82	125	126	**135**	107
10b	82	125	**136**	183	205

The coefficients (B_{xy}) are fit empirically, for each zone separately, using a χ^2 minimization routine in OriginPro 9 [34]. The mass excess can be calculated by combining the microscopic and macroscopic components, i.e. the $\text{SEM}_{F-\text{Spin}}$ and the macroscopic energy that comes from the FRDM. Table 3 contains the fit parameters for F-Spin_{12}. Figure 3 includes the corresponding fits to the SEM_{12} data. From this it is possible to see that the features of shell closures near stability are well reproduced.

The overall standard deviation between F-Spin_{12} and the AME_{12} data is 338 keV. Figure 4, contains the difference between the fit and experimental SEM values on the chart of the nuclides. This additional information can help one determine how well the data has actually been fit. There are only 15 out of 2317 masses which have a discrepancy between F-Spin_{12} and AME_{12} of more than 1.5 MeV. Because of the large uncertainties in some of these measurements, we

Table 2. F-Spin$_{12}$ and F-Spin$_{12S}$ Coefficients and Fit Parameters

Zone	B_{00} x10^3	B_{01} x10^1	B_{02} x10^{-1}	B_{10} x10^2	B_{11} x10^0	B_{12} x10^{-1}	B_{20} x10^1	B_{21} x10^0	B_{22} x10^{-1}	χ^2
1	0.0147900	-0.1452416	0.4285861	0.1183917	-1.6121992	0.5694757	-1.0610863	1.8878219	-0.7900485	0.88
2	-0.0475336	0.7870946	-3.0531705	0.6054538	-8.6012758	3.2322905	-2.4266262	2.9444939	-0.9753579	0.17
3	-0.0741829	0.7367648	-1.7272693	-0.8492452	6.4960763	-1.1991330	-3.4099642	2.4420547	-0.4308491	0.18
4	-0.0863218	0.7171904	-1.4457002	0.7306156	-6.0531135	1.2234365	4.4280193	-3.4529176	0.6652815	0.16
5	-0.0977425	0.5425733	-0.7258019	0.0751298	-0.7473322	0.1320527	0.3513260	-0.2106814	0.0237564	0.12
6	-0.0811950	0.4234495	-0.5236430	0.0831527	-0.6586171	0.1074919	-0.5821897	0.2747766	-0.0346648	0.11
7	-0.2836332	0.9055215	-0.7127516	-0.7886907	2.3032209	-0.1670863	-0.6533741	0.1790153	-0.0125753	0.10
8	-0.1153739	0.3432309	-0.2525416	-0.0865233	0.1532584	-0.0027881	0.6698855	-0.1831231	0.0120209	1.18
9	-1.7106991	3.8622297	-2.1788232	-3.6607297	8.1261257	-0.4526118	-1.7925891	0.3840887	-0.0208027	0.03
10	-0.6157849	1.3008683	-0.6877197	-3.8641512	8.1970897	-0.4339413	-4.9044329	1.0658861	-0.0578951	0.95
1a	-0.0283268	0.6574424	-3.1936856	0.1033252	-3.6748069	2.5282586	-1.4860543	2.5421077	-1.3537825	0.37
1b	-0.0274703	0.4902454	-1.9057283	0.5251396	-8.5107438	3.2539922	-0.0939506	0.8355109	-0.4825100	0.29
8a	-0.3871140	1.2628455	-1.0226552	0.0670634	-0.6962423	0.0953547	0.2088205	-0.0473826	0.0007183	0.04
8b	-0.0261230	0.1187289	-0.1234234	-1.7651592	5.7003851	-0.4617881	6.3602980	-2.0576716	0.1674703	0.08
8c	0.0525327	-0.1335492	0.0857013	0.6845233	-1.8308691	0.1234314	-0.8907357	0.2746192	-0.0209872	0.16
10a	-1.1041726	2.4026883	-1.3075806	0.5074829	-1.7769501	0.1343399	-4.0551190	0.9572352	-0.0569254	0.04
10b	0.0500503	-0.0923226	0.0390522	0.7830141	-1.5869912	0.0793818	-1.9350190	0.3968104	-0.0199591	0.04

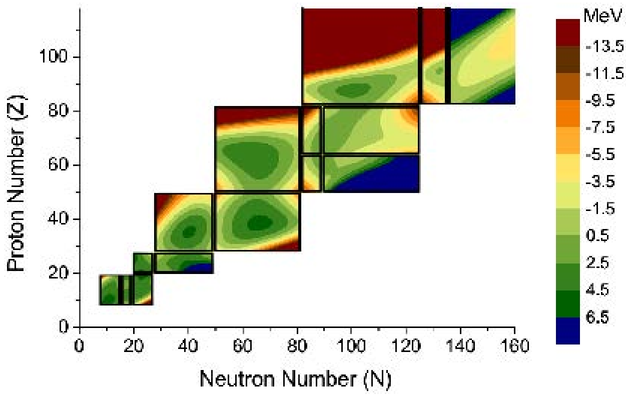

Figure 3. (Color on-line) The predicted SEM using F-Spin$_{12}$ fits summarized in Table 3 using 15 zones.

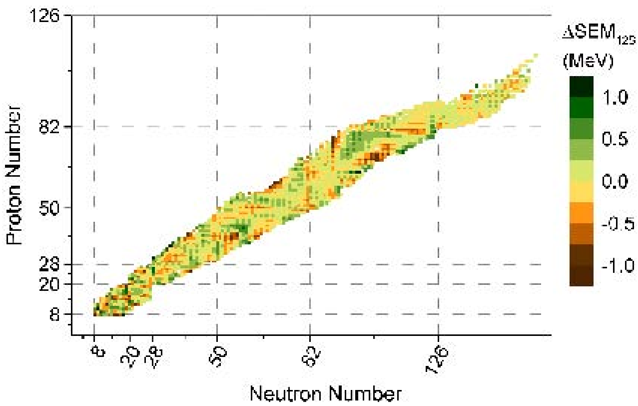

Figure 4. (Color on-line) Difference between the experimental AME$_{12}$ and the F-Spin$_{12}$ fit.

intend to compare the present best fit F-Spin$_{12}$ with a compilation of precision measurements, not all of which have been included in AME$_{12}$.

4 Summary

Simple relationships between SEM and F_0 or P allow one to predict the values of SEM for 15 zones consisting of hundreds of nuclei. While both approaches involve quite simple relationships F-Spin is chosen because of the limitations of P to describe close shells and values of $P < 3$. In most zones, conventional shell closures are sufficient in allowing for a substantial improvement in generating nuclear masses over FRDM, often by a factor of 2. Three zones where this was not the case have been broken into smaller sub-shells resulting in fits, which have standard deviations of about 300 keV.

Comparisons with new mass measurements tabulated in the AME_{12} are occasionally suspect as a result of large experimental uncertainties. Rather, a comparison with high precision JYFLTRAP measurements, indicate that that the fit and predictive ability of the F-Spin remains at about 300 to 400 keV.

The robustness of the extrapolation of the F-Spin fits far from stability is questionable. The maxima in the corners of some zones occur when zones are approximately half full. This amount of information is insufficient for determining location of the turning point which occurs toward the middle of most zones.

The strength in this approach is to predict the masses which can potentially be measured in the next generation of experiment or to fill in missing masses in regions where nearby some data is known. On the basis of obtained mass excess predictions for 20 nuclei which do not have measured masses in AME_{12}, but for which all, or nearly all, of the neighboring values are known, we could propose new precise mass measurements. The ability to interpolate, and make minor extrapolations, makes this a potentially useful tool. Overall, the extrapolation/interpolations from the AME_{12} and F-$Spin_{12}$ are comparable for these nuclei.

Although the zones contain nine parameters which are used to fit them, it should be stressed that there are on average about 150 nuclei, which can be fit by those nine parameters. Furthermore, those nine parameters are able to give comparable, if not better fits, to those nuclei than state of art mass models specifically, [4], [10] and [11]. This approach has substantially fewer parameters than other fits such as the quartic IMME which would require several hundred parameters to achieve fits for the same number of nuclei.

Acknowledgments

AIG is grateful for the support and hospitalities of the Department of Physics of Notre Dame University. This work has been supported by the Bulgarian National Science Fund under contract No. DFNI-E02/6.

References

[1] C.F. von Weizsacker (1935) *Z. Phys.* **96** 431.

[2] H.A. Bethe and R.F. Bacher (1936) *Rev. Mod. Phys.* **8** 82.

[3] M.V. Stoitsov, J. Dobaczewski, W. Nazarewicz, S. Pittel, and D.J. Dean (2003) *Phys. Rev. C* **68** 054312.

[4] S. Goriely, N. Chamel, J.M. Pearson (2010) *Phys. Rev. C* **82** 035804.

[5] Y. Aboussir, J. M. Pearson, A.K. Dutta, and F. Tondeur (1995) *Atomic Data and Nuclear Data Tables* **61** 127.

[6] K.D. Sviratcheva, C. Bahri, A.I. Georgieva, and J.P. Draayer (2004) *Phys. Rev. Lett.* **93** 152501.
[7] A. Bohr, B.R. Mottelson, and D. Pines (1958) *Phys. Rev*. **110** 936.
[8] P. Möller, J.R. Nix, W.D. Myers, and W.J. Swiatecki (1995) *Atomic Data and Nuclear Data Tables* **59** 185.
[9] J. Duflo, A.P. Zuker (1995) *Phys. Rev. C* **52** R23.
[10] J. Mendoza-Temis, J.G. Hirsch, A.P. Zuker (2010) *Nucl. Phys. A* **843** 14-36.
[11] N. Wang, M. Liu (2013) *J. Phys.: Conf. Ser.* **420** 012057.
[12] K. Oyamatsu, K. Iida, H. Koura (2010) *Phys. Rev. C* **82** 027301.
[13] G.T. Garvey, W.J. Gerace, R.L. Jaffe, I. Talmi, and I. Kelson, Rev. Mod. Phys. 41, S1-S80 (1969)
[14] J. Barea, A. Frank, J.G. Hirsch, P. Van Isacker, S. Pittel, V. Velazquez, Phys. Rev. C77 041304(R) (2008).
[15] G.J. Fu, H. Jiang, Y.M., S. Pittel and A. Arima, Phys. Rev. C 82, 034304 (2010).
[16] E.P. Wigner (1957) *Proc. Robert A. Welch Found. Conf. Chem. Res.*, Houston, Texas.
[17] A. Bohr and B. Mottelson (1999) *Nuclear Structure I: Single-Particle Motion*, World Scientific.
[18] D.H. Wilkinson (1964) *Phys. Rev. Lett.* **13** 571-573.
[19] W. Beneson, E. Kashy (1979) *Rev. Mod. Phys*. **51** 527.
[20] R. E. Tribble, R.A. Kenefick, and R.L. Spross (1976) *Phys. Rev. C* **13** 50-54.
[21] E. Norman, L. Schroeder, and G. Wozniak, Eds. (2002) *New Mass Measurements with the ISOLTRAP Spectrometer*, vol. 610 of American Institute of Physics Conference Series.
[22] R.F. Casten (1990) *Nuclear Structure From a Simple Perspective*, Oxford.
[23] S. Drenska, A. Georgieva, V. Gueorguiev, R. Roussev, and P. Raychev (1995) *Phys. Rev. C* **52** 1853.
[24] A. Georgieva, M. Ivanov, P. Raychev and R. Roussev (1989) *Int. J. Theor. Phys*. **28** 769.
[25] A. Arima, T. Otsuca, F. Iachello and I. Talmi (1977) *Phys. Lett.* **66B** 205; J.P. Elliott, (1985) *Rep. Prog. Phys.* **48** 171.
[26] R.F. Casten (1985) *Nucl. Phys.* **A443** 1.
[27] R.F. Casten, D.S. Brenner, and P.E. Haustein (1987) *Phys. Rev. Lett*. **58** 658.
[28] P.E. Haustein, D.S. Brenner and R.F. Casten (1988) *Phys. Rev. C* **38** 1.
[29] G. Audi, M. Wang, A. Wapstra, F. Kondev, M. MacCormick, X. Xu, and B. Pfeiffer (2012) *Chinese Phys. C* **36** 1287.
[30] A. Teymurazyan, A. Aprahamian, and A. Georgieva (2004) *BgNS Transactions* **9** 165; A. Teymurazyan, A. Aprahamian, and A.I. Georgieva (2002) In *Proceedings of the International Conference on Nuclear Structure, "Mapping the Triangle"*, Wyoming, May 22-25, 2002, eds. A. Aprahamian, J. Cizewski, S. Pittel and N. Zamfir, AIP Conference Proceedings **638** 271-273.
[31] O. Sorlin, M.-G. Porquet (2008) *Prog. Part. Nucl. Phys.* **61** 602-673.
[32] T. Otsuka (2013) *Phys. Scripta* **T152** 014007.
[33] R.F. Casten, D.D. Warner, D.S. Brenner, and R.L. Gill (1981) *Phys. Rev. Lett*. **47** 1433-1436.
[34] OriginPro 9, online at: http://www.originlab.com. ©2012 OriginLab Corporation.